Volume 1 | Number 1 | Jan 2013 | Pages 1–100

MedChemComm

www.rsc.org/medchemcomm

pDOS

ROYAL SOCIETY
OF CHEMISTRY

EFMC
European Federation
for Medicinal Chemistry

ROYAL SOCIETY
OF CHEMISTRY

www.rsc.org/medchemcomm

Journal Name

Dynamic Article Links ▶

ARTICLE TYPE

Discovery of a series of 2-(pyridinyl)pyrimidines as potent antagonists of GPR40

Michael J. Waring,*[a] David J. Baker, Stuart N. L. Bennett, Alexander G. Dossetter, Mark Fenwick, Rob Garcia, Jennie Georgsson, Sam D. Groombridge, Susan Loxham, Philip A. MacFaul, Katie G. Maskill, David Morgan, Jenny Morrell, Helen Pointon, Graeme R. Robb, David M. Smith, Stephen Stokes and Gary Wilkinson

A series of 2-(pyridinyl)pyrimidines were identified as potent GPR40 antagonists. Despite significant challenges related to improving the combination of potency and lipophilicity within the series, the compounds were optimised to identify a suitable *in vivo* probe compound, which was confirmed to exhibit pharmacology consistent with GPR40 antagonism.

GPR40 (FFAR1) is a family A GPCR which is highly and selectively expressed on the human insulin secreting beta-cells of the pancreas.[1] When activated, the receptor is coupled to the Gq signal transduction mechanism and mediates an increase in intracellular calcium and the secretion of insulin. Insulin secretion only occurs when glucose concentrations are high and thus GPR40 agonists have been considered good candidates for treatment of type 2 diabetes without risk of hypoglycaemia. This hypothesis has been vindicated in clinical trials with Fasiglifam, TAK-875 (**Fig. 1**), Takeda's GPR40 agonist,[2] although the recent failure of the compound in Phase III trials has given rise to safety concerns based on hepatotoxicity.[3] The naturally occurring ligands for GPR40 are thought to be saturated fatty acids which have long been considered to have a chronic lipotoxic effect on the beta-cell.[4] Thus an alternative hypothesis would be that if the lipotoxic effects of saturated fatty acids were mediated by GPR40 then an antagonist approach, whilst being contraindicated acutely (lowering of insulin secretion), would in the long run be a beneficial therapy. Data from GPR40 deleted mice and transgenic over expression of GPR40 have yielded controversial results. Studies have shown a benefit of GPR40 knockout on the metabolic defects of high fat fed mice[5,6] and a detrimental effect of beta-cell specific over expression of GPR40. However, both of these claims have been countered.[7-11]

It has been shown recently that human islets cultured long term in the presence of a GPR40 antagonist (ANT203, **Fig. 1**) showed a number of beneficial effects, including inhibition of the detrimental effects of palmitate on glucose stimulated insulin secretion and insulin content,[12] although perhaps contrary results have also been described.[13-15] ANT203 has some undesirable structural properties containing a non-druglike hydrazone group as well as very high $logD_{7.4}$ resulting in low solubility and very poor bioavailability. Hence, the programme to identify more drug-like GPR40 antagonist compounds described herein was initiated, with the goal of testing the GPR40 lipotoxicity hypothesis *in vivo*. A number of groups have also disclosed GPR40 antagonists in the literature.[16-19]
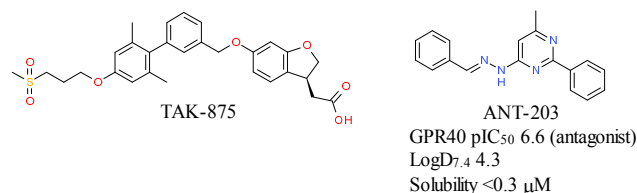

Fig. 1 Structures of TAK-875 and ANT203

TAK-875

ANT-203
GPR40 pIC_{50} 6.6 (antagonist)
$LogD_{7.4}$ 4.3
Solubility <0.3 μM

In order to identify antagonists of GPR40, a high throughput screen of the AstraZeneca compound collection was carried out, screening in HEK cells stably transfected with GPR40 stimulated with elaidic acid and measuring the secondary messenger IP1 by time resolved fluorescence as an endpoint. Active compounds were selected for IC_{50} determination and confirmation of activity using calcium flux as an alternative end point. This exercise identified pyrimidine **1** (**Fig. 2**) as a moderately potent (pIC_{50} 6.2) GPR40 antagonist with reasonable lipophilicity ($logD_{7.4}$ 2.8).

1
GPR40 pIC_{50} 6.2
LogD 2.8

2
GPR40 pIC_{50} 6.1
LogD 2.7
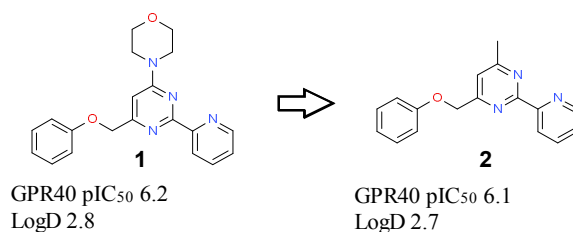
Fig. 2 Initial hit and removal of morpholine
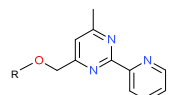
Compound **1** was originally synthesised as part of a programme to identify inhibitors of the human target of rapamycin.[20] As a consequence, it carried some weak activity against lipid kinases such as phosphatidyl inositol-3-kinase (pIC_{50} 4.2 and 4.8 for the α and β subtypes respectively). Lipid kinases of this type are known to make a critical hydrogen bonding interaction between a backbone NH in the protein and the morpholine oxygen.[21] Initial exploration of analogues of **1** revealed that the morpholine could be replaced with a methyl group (**2**) with retained GPR40

MedChemComm Accepted Manuscript

antagonist activity and equivalent lipophilicity (pIC$_{50}$ 6.1, logD$_{7.4}$ 2.7) and thus removing concerns about lipid kinase activity during optimisation.

The structure activity relationships of **2** were explored with a view to improving potency and, ideally, reducing lipophilicity [improving lipophilic ligand efficiency (LLE, pIC$_{50}$-logD$_{7.4}$)].[22] Exploration of the pyridine substituent at the pyrimidine 2-position of **2** suggested that the 2-pyridyl was optimal. For instance other pyridine isomers had reduced potency (data not shown).

A systematic exploration of substituent effects on the pendant phenyl group was then carried out (**Table 1**). This revealed a strong link between potency and lipophilicity in this region. Potency could be increased by incorporation of a chloro-substituent with a concomitant increase in logD$_{7.4}$. 2-substitution (**3**) appeared better marginally better than 3- or 4- substitution (**4** and **5**) having a pIC$_{50}$ of 6.5 and a logD$_{7.4}$ of 3.4 and, hence, a slight increase in LLE relative to phenyl derivative **2** (0.4 units). Incorporation of polar substituents methoxy- (**6**, **7** and **8**), cyano- (**9**, **10** and **11**), acetamido- (**12**, **13** and **14**) and methanesulfonyl (**15**, **16** and **17**) led to reduced potency in all cases. Slight benefits in potency could be achieved with fluoro-substitution, most notably again at the 2-position [pIC$_{50}$ 6.4, 6.1, 6.2 for 2-, 3- and 4- isomers (**18**, **19** and **20**) respectively] without significant increases in lipophilicity (logD$_{7.4}$ 2.9, 3.1 and 3.0). As a result, the 2-fluorophenyl derivative **18** showed an improvement in LLE of 0.8 log units relative to phenyl **2** (3.5 vs. 2.7). Additional exploration of this group by replacement with aromatic or aliphatic heterocycles showed diminished potency and no improvement in LLE (see ESI).

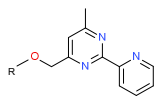**Table 1** Exploration of substitution of the phenyl ring

R	pIC$_{50}$	logD$_{7.4}$	pIC$_{50}$- logD$_{7.4}$
Ph (**2**)	6.1	3.4	2.7
2-chlorophenyl (**3**)	6.5	3.4	3.1
3-chlorophenyl (**4**)	6.4	3.7	2.7
4-chlorophenyl (**5**)	6.6	3.7	2.9
2-methoxyphenyl (**6**)	5.7	2.5	3.2
3-methoxyphenyl (**7**)	5.7	2.9	2.8
4-methoxyphenyl (**8**)	5.1	2.8	2.3
2-cyanophenyl (**9**)	5.0	2.7	2.3
3-cyanophenyl (**10**)	5.6	2.7	2.9
4-cyanophenyl (**11**)	4.5	2.6	1.9
2-acetamidophenyl (**12**)	<4.4	1.6	-
3-acetamidophenyl (**13**)	<4.4	2.1	-
4-acetamidophenyl (**14**)	<4.4	1.9	-
2-methanesulfonyl (**15**)	<4.4	1.5	-
3-methanesulfonyl (**16**)	<4.4	1.7	-
4-methanesulfonyl (**17**)	<4.4	1.5	-
2-fluorophenyl (**18**)	6.4	2.9	3.5
3-fluorophenyl (**19**)	6.1	3.1	3.0
4-fluorophenyl (**20**)	6.2	3.0	3.2

Given the relationship between potency and lipophilicity observed in this region, it appeared that the best strategy to optimise LLE was to exploit the apparent benefit of fluorination. Accordingly, combinations of di- and tri-fluorination patterns were explored (**Table 2**). All combinations of difluorination (**21**,

22 and **23**) appeared to be similar in potency to the 2-fluoro derivative **18** with slight increases in lipophilicity (reduced LLE). For the trifluoro derivatives, the 2,3,4-isomer **24** appeared to possess the best balance of potency and lipophilicity (pIC$_{50}$ 6.6, logD$_{7.4}$ 3.3) with other combinations (**25–29**) showing slightly reduced potency, increased lipophilicity or both. Accordingly, 2,3,4-trifluoro derivative **24** was identified as the optimal fluorination pattern. This represented an increase in potency from the initial phenyl derivative **2** of 0.5 log units with no change in lipophilicity. Whilst these changes are small, they are meaningful; the potency values for phenyl **2**, 2-fluorophenyl **18** and 2,3,4-trifluorophenyl **24** derivatives were shown to be statistically significantly different to each other (see ESI).
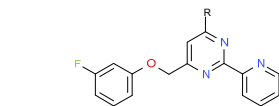
Table 2 Effect of multiple phenyl ring fluorine substitutions

R	pIC$_{50}$	logD$_{7.4}$	pIC$_{50}$- logD$_{7.4}$
2,3-difluorophenyl (**21**)	6.4	3.2	3.2
2,4-difluorophenyl (**22**)	6.4	3.1	3.3
3,4-difluorophenyl (**23**)	6.3	3.2	3.1
2,3,4-trifluorophenyl (**24**)	6.6	3.3	3.3
2,3,5-trifluorophenyl (**25**)	6.3	3.4	2.9
2,3,6-trifluorophenyl (**26**)	5.8	3.1	2.7
2,4,5-trifluorophenyl (**27**)	6.4	3.2	3.2
2,4,6-trifluorophenyl (**28**)	5.9	3.2	2.7
3,4,5-trifluorophenyl (**29**)	6.4	3.4	3.0

At the same time, replacement of the pyrimidine 4-methyl substituent was explored. Initial analogues were prepared with a 3-fluorophenyl as the ether substituent (**Table 3**). This revealed that oxygen and nitrogen links (the latter precedented from the initial hit) were tolerated although both the methoxy- (**30**) and dimethylamino- (**32**) derivatives showed slightly reduced potency with increased lipophilicity and hence reduced LLE (2.3 and 2.2) respectively relative to 3.0 for methyl derivative **19**). Potency could be increased on both the ether and amine linked series with larger and more lipophilic alkyl substituents such as ethyl (**31** and **33**) and isopropyl (**34**).

Table 3 Initial replacements of the pyrimidine 4–methyl substituent

R	pIC$_{50}$	logD$_{7.4}$	pIC$_{50}$-logD$_{7.4}$
-Me (**19**)	6.1	3.1	3.0
-OMe (**30**)	5.9	3.6	2.3
-OEt (**31**)	6.6	4.1	2.5
-NMe$_2$ (**32**)	5.8	3.6	2.2
-NHEt (**33**)	6.2	3.9	2.3
NH^{i}Pr (**34**)	7.0	4.3	2.7

Subsequently, these observations were further developed in the optimised 2,3,4-trifluorophenyl ether series (**Table 4**). In the nitrogen linked series, it was discovered that a dimethylazetidine substituent (**35**) gave a significant potency increase (pIC$_{50}$ 7.6

relative to 6.6 for methyl **24**) in line with the lipophilicity increase (constant LLE). Incorporation of polar substituents such as hydroxyl (**36**), oxetanyl (**37**), and methanesulfonylmethyl (**38**) at the azetidine-3-position all served to reduce the logD but at the cost of potency resulting in LLE values that were all less than that of the methyl derivative **24**. The best balance was observed with the 3-cyano-3-methylazetidine derivative **39** (pIC$_{50}$ 6.8, logD$_{7.4}$ 3.3).

In the oxygen linked series, it was observed that further potency benefits could be obtained with lipophilic substituents. The 2,2,2-trifluoroethyl derivative **40** was the most potent compound (pIC50 8.1) although, again, with immeasurably high logD$_{7.4}$. The cyclobutylmethylether **41** showed similar potency with lower logD$_{7.4}$ and with more scope to introduce polar substituents to reduce the lipophilicity. The oxetanyl derivative **42** showed reduced potency and LLE relative to the cyclobutyl. Incorporation of a methyl group at the oxetane 3-position (**43**) increased potency significantly with an increase in LLE despite the increase in logD7.4 and suggested that further substitution may be possible at this position. Changing the methyl group for methoxy (**44**) served to reduce lipophilicity and potency whereas a cyanomethyl substituent (**45**) retained potency relative to the unsubstituted oxetane with a reduction in logD and thus slightly increased LLE (3.1 relative to 2.8 for the unsubstituted oxetane). The best balance (highest LLE) within this subseries was displayed by the 3-fluorooxetane derivative **46** (pIC$_{50}$ 7.2, logD$_{7.4}$ 4.0).

**Table 4** Further changes to the pyrimidine 4-methyl substituent

R	pIC$_{50}$	logD$_{7.4}$	pIC$_{50}$- logD$_{7.4}$
-Me (**24**)	6.6	3.3	3.3
(**35**)	7.6	4.3	3.3
(**36**)	5.5	2.8	2.7
(**37**)	6.3	3.3	3.0
(**38**)	5.2	2.9	2.3
(**39**)	6.8	3.3	3.5
(**40**)	8.1	>4.9	-
(**41**)	7.9	4.5	3.4
(**42**)	6.5	3.7	2.8
(**43**)	7.1	4.0	3.1
(**44**)	6.3	3.5	2.8
(**45**)	6.4	3.3	3.1
(**46**)	7.2	4.0	3.2

Whilst these examples illustrate that optimisation of LLE in this series is challenging, compounds **39** and **46** show the best balance

of potency and lipophilicity and show improved potency and LLE relative to starting point **2** (0.7 and 1.1 log increases in potency and 0.8 and 0.5 unit increases in LLE for **39** and **49** respectively compared to **2**, see also **Fig. 5**).

Subsequently, a crystal structure of GPR40 bound to the allosteric agonist TAK-875 has been obtained.[23] This shows that the ligand binds in an unusual allosteric pocket, formed between transmembrane helices 3, 4 and 5. Analysis of the crystal structure revealed no other pocket large enough to accommodate compounds from our series. It was therefore hypothesised that the compounds reported here bind in the same site as TAK-875, but in such a way as to cause antagonism rather than agonism. The structure is appropriate for antagonist binding as it has crystallised in the inactive form.

In order to better understand ligand binding to GPR40 the crystal structure was subjected to an energetic analysis using the 3D-RISM method[24] implemented in the MOE software package.[25] The analysis identified predicted locations of water molecules within the binding site and their associated stability as free-energy of binding (**Fig. 3a**). Two predicted water sites were identified within the pocket, close to the carboxylic acid of the ligand, which were not, in reality, occupied in the crystal structure. These sites can also be interpreted as locations of potential ligand-protein interactions and these were selected as pharmacophore points (any ligand atom) for docking. An induced-fit docking protocol was used where, after initial pose generation, protein side-chains within 6Å of the ligand were optimised along with the ligand. Compound **39** was docked using this method and it was observed that both pharmacophore sites were occupied with polar groups from the ligand (**Fig. 3b**). The pyridine group was observed to form a hydrogen bond to Arg183, though the geometry was sub-optimal. The cyano group made no hydrogen bonds, but also contacted Arg183. Furthermore, the lipophilic interactions of the phenyl group in TAK-875 were replicated nicely by the phenyl of **39**. In order to accommodate the pyridine ring, Leu171 rotated and opened up a large sub-pocket towards transmembrane helix 2. This marked the most significant departure from the binding mode of TAK-875 and so it could be proposed that occupying this pocket is the reason for the observed antagonism of these compounds, rather than the agonism of TAK-875.
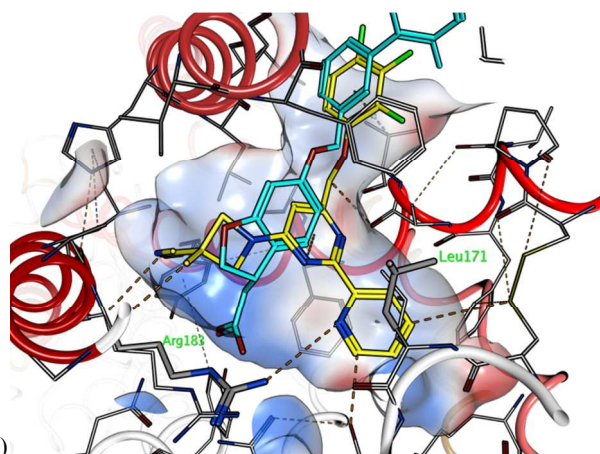

a)

b)
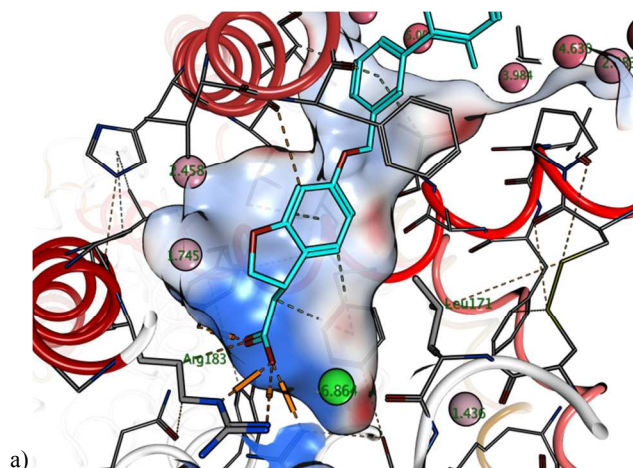
Fig. 3 (a) 3D-RISM solvent analysis of GPR40 in complex with TAK-875 (PDB=4PHU[23]). Spheres indicate predicted water molecule sites where the numeric label indicates the ΔG of binding (kcal/mol): green
5 (negative ΔG) is stable, red (positive ΔG) is unstable. **(b)** GPR40 structure with compound **39** bound. Leu171 and Arg183 have both moved from their original positions (also drawn) during the induced-fit docking protocol

The 3D model also agrees with the observation that much of the
10 SAR is lipophilicity driven. The binding site shows very little hydrophilic character (blue/red coloured surface in **Fig. 2**) with the exception of potential interactions with Arg183 and nearby residues at one end of the binding site. Binding affinity throughout the rest of the molecule is largely driven by non-polar
15 contacts.

Despite their non-ideal lipophilicity,[26] compounds **24**, **39** and **46** all showed reasonable ADMET properties (**Table 5**) although **39** and **46** had poorer solubility and some hERG activity. The compounds showed moderate intrinsic clearance in rat
20 hepatocytes although values were higher in human microsomes. Consistent with the rat *in vitro* data, all three compounds had moderate rat clearance and **24** and **39** showed good bioavailability and fraction absorbed in rat pharmacokinetic studies, resulting in sufficient oral exposure to be suitable as *in*
25 *vivo* probes. In addition, **39** had comparable activity against the rat and mouse GPR40 isoforms and had no measurable activity against the related fatty acid receptor GPR43 (FFAR2) and a relatively benign secondary pharmacology profile [only 1 target (pig Na^+/K^+ ATPase)out of 144 tested showed potency greater
30 than 1 μM, for further details see ESI] making it a suitable *in vivo* probe.

Table 5 Profiles of **24**, **39** and **46**

		-Me		
	R=	**(24)**	**(39)**	**(46)**
GPR40 pIC$_{50}$ hu / rat		6.6 / 6.7	6.8 / 7.2	7.2 / 7.5
logD$_{7.4}$		3.3	3.3	4.0
Solubility / μM		22	2.9	2.9
%free (rat / hu)		6.3 / 3.0	5.6 / 4.8	1.7 / 1.5
hERG pIC$_{50}$		< 4.5	5.0	5.2
Cl$_{int}$ (rat hep / hu mics) / mLmin^{-1}10^6		17 / 57	26 / 52	72 / 56
Rat Cl (Cl$_u$) / mLmin^{-1}kg^{-1}		24 (380)	30 (540)	19 (1100)
Rat V$_{ss}$ / Lkg^{-1}		2.3	3.0	1.4
Rat F (F$_{abs}$) %		39 (59)	32 (56)	12 (16)

To confirm that compound **39** effects GPR40 antagonism *in vivo*,
35 it was tested in a β$_3$-agonist challenge (lipolysis) model in the insulin resistant Zucker fa/fa rats.[7] Male Zucker rats (n=8/group) were dosed with either vehicle (PVP/SDS 5 mg/kg, p.o.) or **39** at 80 mg/kg with or without β$_3$-agonist pre-treatment 30 minutes prior to dosing. 4 hours post dosing, plasma samples were
40 collected and non-esterified fatty acids (NEFA) and insulin levels were measured using ELISA assays. The data show that, in the absence of the β$_3$-agonist challenge, plasma NEFA concentration remained at a basal level (**Fig. 4a**) and that the GPR40 antagonist did not alter insulin secretion compared with vehicle (**Fig. 4b**).
45 However, in the presence of the β$_3$-agonist the plasma NEFA levels of vehicle treated animals increased by 6-fold which produced a concomitant fatty acid driven insulin secretion 3.5-fold above the vehicle treated animals without a β$_3$-challenge. The GPR40 antagonist significantly inhibited NEFA driven
50 insulin secretion by ~70% (P<0.01), such that it was only 1.7-fold above the non β$_3$-challenge state. These data suggest that GPR40 antagonists can reduce fatty acid stimulated insulin secretion, which may be therapeutically beneficial for hyperinsulinaemic and insulin resistant states where fatty acid potentiation of
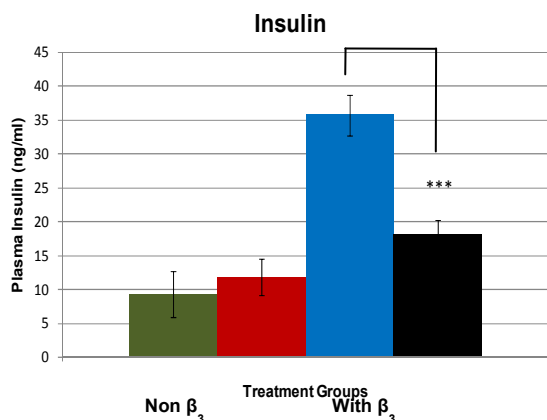55 glucose stimulated insulin secretion (GSIS) is a major source of raised insulin levels.

a)
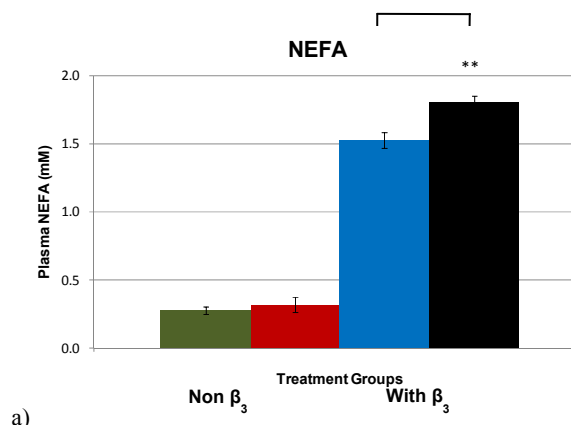
Fig. 4 Effect of **39** on β3-agonist stimulated NEFA (a) and insulin (b) levels in Zucker fa/fa rats. Vehicle non- β3-agonist (green), **39** without β3 agonist (red), vehicle with β3-agonist (blue), **39** with β3-agonist (black).

Conclusions

The structure activity relationships described here highlight the lipophilic nature of the GPR40 binding pocket and the challenges that compound optimisation in such a situation presents. Nevertheless, incremental improvements were possible by systematic structural exploration, most notably by exploiting the isolipophilic changes of multiple fluorine substitutions on the phenyl ring. This work allowed the identification of compounds suitable as *in vivo* probes, most notably compound **39**, although the scope for further optimisation of this series is questionable. Further studies describing the pharmacological evaluation of **39**, assessing the consequences of GPR40 antagonism *in vivo*, will be the subject of further publications.

The use of LLE to assess the effect of structural modifications on potency in the context of changes in lipophilicity was useful. The use of composite parameters such as LLE has recently been the subject of controversy[27] with justified points concerning the thermodynamic and mathematical basis for LLE (potency offsetting) being raised.[28] In this study, the use of LLE is justifiable from this perspective, since the compounds show a very clear relationship between pIC_{50} and $logD_{7.4}$ values and the line of best fit in the corresponding scatter plot has a gradient of unity (**Fig. 5**). It might be hypothesised that this is what would be expected for a series in which affinity is driven by lipophilic interactions.
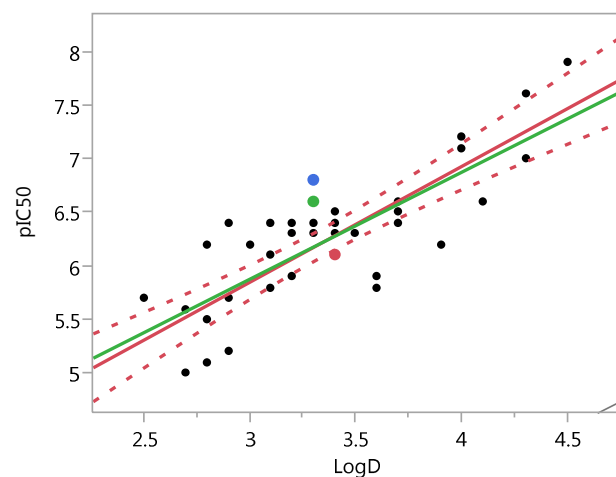

Fig. 5 LLE plot for the series. Red line shows the line of best fit ($pIC_{50}=2.6+1.1logD_{7.4}$, $r^2=0.65$), red dotted lines show the 95% confidence in the fit, green line is the line of slope = 1. Key compounds are highlighted **2** (red), **24** (green), **39** (blue).

Data obtained from a β_3-agonist challenge carried out using the GPR40 knockout mouse demonstrated that potentiation of GSIS by GPR40 contributes to ~50% of all insulin secretion under hyperlipidaemic conditions. A reduction in insulin levels from 35 ng/mL to 18ng/mL during the β_3– agonist challenge suggests that the antagonist **39** was able to completely inhibit the NEFA driven potentiation of GSIS pharmacologically, in line with the maximum contribution this mechanism can make to GSIS implied by the knockout mouse data.[8] Further studies on the pharmacology of these compounds will be reported in due course.

Notes and references

a AstraZeneca, Mereside, Alderley Park, Macclesfield, Cheshire, UK.; Tel: +44 (0)1625 230942; E-mail: mike.j.waring@astrazeenca.com

† Electronic Supplementary Information (ESI) available: Datatables for additional compounds, experimental details for the biological assays and synthesis of **39**, tests for statistical differences in potency values, further details of the molecular modelling and the secondary pharmacology profile of **39**. See DOI: 10.1039/b000000x/

1   A. D. Mancini, V. Poitout, *Trends Endocrin. Met.* 2013, **24**, 398.
2   C. F. Burant, P. Viswanathan, J. Marcinak, C. Cao, M. Vakilynejad, B. Xie, E. Leifke, *Lancet* 2012, **379**, 1403.
3   A. D. Mancini, V. Poitout, *Diabetes, Obes. Metab.*, doi: 10.1111/dom.12442
4   M. Prentki, E. Joly, W. El-Assaad, R. Roduit, *Diabetes* 2002, **51**, S405.
5   P. Steneberg, N. Rubins, R. Bartoov-Shifman, M. D. Walker, H. Edlund, *Cell Metab.* 2005, **1**, 245.
6   R. Brownlie, R. M. Mayers, J. A. Pierce, A. E. Marley, D. M. Smith, *Biochem. Soc. Trans.* 2008, **36**, 950.
7   H. Lan, L. M. Hoos, L. Liu, G. Tetzloff, W. Hu, S. J. Abbondanzo, G. Vassileva, E. L. Gustafson, J. A. Hedrick, H. R. Davis, *Diabetes* 2008, **57**, 2999.
8   M. G. Latour, T. Alquier, E. Oseid, C. Tremblay, T. L. Jetton, J. Luo, D. C. Lin, V. Poitout, *Diabetes* 2007, **56**, 1087.
9   K. Nagasumi, R. Esaki, K. Iwachidow, Y. Yasuhara, K. Ogi, H. Tanaka, M. Nakata, T. Yano, K. Shimakawa, S. Taketomi, K. Takeuchi, H. Odaka, Y. Kaisho, *Diabetes* 2009, **58**, 1067.
10 C. P. Tan, Y. Feng, Y.-P. Zhou, G. J. Eiermann, A. Petrov, C. Zhou, S. Lin, G. Salituro, P. Mainke, R. Mosley, T. E. Akiyama, M. Einstein, S. Kumar, J. P. Berger, S. G. Mills, N. A. Thornberry, L. Yang, A. D. Howard, *Diabetes*, 2008, **57**, 2211.

MedChemComm Accepted Manuscript

11 M. Kebede, T. Alquier, M. G. Latour, M. Semache, C. Tremblay, V. Poitout, *Diabetes*, 2008, **57**, 2432.

12 H. Kristinsson, D. M. Smith, P. Bergsten, E. Sargsyan, *Endocrinology*, 2013, **154**, 4078.

13 R. Wagner, G. Kaiser, F. Gerst, E. Christiansen, M. E. Due-Hansen, M. Grundmann, F. Machicao, A. Peter, E. Kostenis, T. Ulven, A. Fritsche, H.-U. Häring, S. Ullrich, *Diabetes*, 2013, **62**, 2106.

14 P. Wu, L. Yang, X. Shen, *Biochem. Biophys. Res. Commun.* 2010, **403**, 36.

15 Y. Zhang, M. Xu, S. Zhang , L. Yan, C. Yang, W. Lu, Y. Li, H. Cheng, *J. Mol. Endocrinol.* 2007, **38**, 651.

16 Y. Zhao, J. Liao, *Heterocycles*, 2011, **83**, 1145; X. Zhang, G. Yan, Y. Li, W. Zhu, H. Wang, *Biomed. Pharmacol. J.* 2010, **64**, 647.

17 H. Hu, L. Y. He, Z. Gong, N. Li, Y. N. Lu, Q. W. Zhai, H. Liu, H. L. Jiang, W. L. Zhu, H. Y. Wang, *Biochem. Biophys. Res. Commun.* 2009, **390**, 557.

18 P. S. Humphries, J. W. Benbow, P. D. Bonin, D. Boyer, S. D. Doran, R. K. Frisbie, D. W. Piotrowski, G. Balan, B. M. Bechle, E. L. Conn, K. J. Dirico, R. M. Oliver, W. C. Soeller, J. A. Southers, X. Yang. *Bioorg. Med. Chem. Lett.* 2009, **19**, 2400.

19 C. P. Briscoe, A. J. Peat, S. C. McKeown, D. F. Corbett, A. S. Goetz, T. R. Littleton, D. C. McCoy, T. P. Kenakin, J. L. Andrews, C. Ammala, J. A. Fornwald, D. M. Ignar, S. Jenkinson, *Br. J. Pharmacol.* 2006, **148**, 619.

20 K. G. Pike, M. R. V. Finlay, S. M. Fillery, A. P. Dishington, PCT Int. Appl. WO2007080382.

21 M. R. V. Finlay, D. Buttar, S. E. Critchlow, A. P. Dishington, S. M. Fillery, E. Fisher, S. C. Glossop, M. A. Graham, T. Johnson, G. M. Lamont, S. Mutton, P. Perkins, K. G. Pike, A. M. Slater, *Bioorg. Med. Chem. Lett*. 2012, **22**, 4163.

22 A. L. Hopkins, G. M. Keserü, P. D. Leeson, D. C. Rees, C. H. Reynolds, *Nat. Rev. Drug Discov.* 2014, **13**, 105.

23 A. Srivastava, J. Yano, Y. Hirozane, G. Kefala, F. Gruswitz, G. Snell, W. Lane, A. Ivetac, K. Aertgeerts, J. Nguyen, A. Jennings, K. Okada, *Nature* 2014, **513**, 124.

24 D. Chandler, H. C. Anderson, *J. Chem. Phys.* 1972, **57**, 1930.

25 http://www.chemcomp.com/MOE-Molecular_Operating_Environment.htm

26 M. J. Waring, *Expert Opin. Drug Discov.* 2010, **5**, 235.

27 M. D. Schultz, *Bioorg. Med. Chem. Lett.* 2013, **23**, 5980.

28 P. W. Kenny, A. Leitão, C. A. Montanari, *J. Comput. Aided Mol. Des*. 2014, **28**, 699.

MedChemComm Accepted Manuscript